arXiv:1411.2644v1 [cond-mat.supr-con] 10 Nov 2014

Exact correlation functions in the cuprate pseudogap phase: combined effects of charge order and pairing

Rufus Boyack, Chien-Te Wu, Peter Scherpelz, and K. Levin

[1] *James Franck Institute, University of Chicago, Chicago, Illinois 60637, USA*

(Dated: November 12, 2014)

There is a multiplicity of charge ordered, pairing-based or pair density wave theories of the cuprate pseudogap, albeit arising from different microscopic mechanisms. For mean field schemes (of which there are many) we demonstrate here that they have precise implications for two body physics in the same way that they are able to address the one body physics of photoemission spectroscopy. This follows because the full vertex can be obtained exactly from the Ward-Takahashi identity. As an illustration, we present the spin response functions, finding that a recently proposed pair density wave (Amperean pairing) scheme is readily distinguishable from other related scenarios.

Introduction.– A number of theories associated with the cuprate pseudogap phase have recently been suggested, based on now widely observed charge order [1–4]. While the underlying physics may be different, what emerges rather generally are BCS-based pairing theories of the normal state with band-structure reconstruction [5–7]. Distinguishing between theories has mostly been based on angle resolved photoemission spectroscopy (ARPES) [8]. However the majority of data available for the cuprates involves two particle properties: appearing for example, in the optical absorption [9], diamagnetism [10], quasi-particle interference in STM [11], neutron [4, 12, 13] and inelastic x-ray scattering in the charge [3] and spin [14] sectors.

In this paper we use the Ward-Takahashi identity (WTI) [15, 16] to develop precise two body response functions for these pairing based pseudogap theories. Such exact response functions make it possible to address two particle cuprate experiments, including the list above, from the perspective of many different theories. As an illustration, we compute the spin-spin correlation functions relevant to neutron scattering in three pseudogap scenarios. That the response functions analytically satisfy the f-sum rule provides the confidence that there are no missing diagrams or significant numerical inaccuracies. By comparing the Amperean pairing scheme [6], and that of Yang, Rice and Zhang [7] with a simple d-wave pseudogap scenario, we find that the first of these leads to a relatively featureless neutron cross section in contrast to the peaks (at and near the antiferromagnetic wave vector), found for the other two.

In this Amperean pairing scheme [6] the mean field self energy is

$$\Sigma_{pg}(K) = \frac{\Delta_1^2}{\omega + \xi_{\mathbf{k}-\mathbf{p}} - \frac{\Delta_2^2}{\omega - \xi_{\mathbf{k}-2\mathbf{p}}}} + \frac{\Delta_2^2}{\omega + \xi_{\mathbf{k}+\mathbf{p}} - \frac{\Delta_1^2}{\omega - \xi_{\mathbf{k}+2\mathbf{p}}}} + \frac{C_1^2}{\omega - \xi_{\mathbf{k}+2\mathbf{p}} - \frac{\Delta_1^2}{\omega + \xi_{\mathbf{k}+\mathbf{p}}}} + \frac{C_2^2}{\omega - \xi_{\mathbf{k}-2\mathbf{p}} - \frac{\Delta_2^2}{\omega + \xi_{\mathbf{k}-\mathbf{p}}}}. \quad (1)$$

We single this particular theory out as an example which is complex and therefore somewhat more inclusive. In Eq. (1) $\Sigma_{pg}(K)$ is expressed in terms of two different finite momentum ($\mathbf{p}$) pseudogaps, $\Delta_1 \equiv \Delta_{\mathbf{p}}$ and $\Delta_2 \equiv \Delta_{-\mathbf{p}}$. In addition we have introduced charge density wave (CDW) amplitudes C_1 and C_2. From the self energy, the full (inverse) Green's function can be deduced: $G^{-1}(K) \equiv G_0^{-1}(K) - \Sigma_{pg}(K) = \omega - \xi_{\mathbf{k}} - \Sigma_{pg}(K)$. This then determines the renormalized band-structure, which can be compared with ARPES experiments. One can similarly add other mean field contributions such as that related to an SDW [17].

It is observed from Eq. (1) that in the Amperean pairing case a BCS-like self energy appears in a continued fraction form within the self energy itself. There are analogies with the approach of Yang, Rice and Zhang (YRZ) [7] in the limit that only one gap term is present, say Δ_1, and when the CDW ordering is absent. Importantly, this single gap self energy involves two types of dispersion relations, so that the pairing term leads to pockets or a reconstruction of the band-structure. For a simpler d-wave pseudogap, with a single gap model, both of these dispersion relations are taken to be the same, as was studied microscopically [18] and phenomenologically [19]. A central contribution of this paper is to show how, via two particle properties, important distinctions between these three different pseudogap theories can be established.

While it is argued to be appropriate for the pseudogap phase [6], the self energy of Eq. (1) is indistinguishable from that of a superconducting state. It is important, then, to ensure that this form for Σ_{pg} does not correspond to an ordered phase. Phase fluctuations have been phenomenologically invoked [5, 6] to destroy order. Regardless of this phenomenology there is a quantitative constraint to be satisfied: the absence of a Meissner effect above T_C implies that the zero frequency and zero momentum current-current correlation function satisfies $\overleftrightarrow{P}(0) = -\left(\frac{\overleftrightarrow{n}}{m}\right)_{\rm dia} \equiv 2\sum_K \frac{\partial^2 \xi_{\mathbf{k}}}{\partial \mathbf{k} \partial \mathbf{k}} G(K)$, so that there is a precise cancellation

between the diamagnetic and paramagnetic current-current correlation functions in the normal state.

Performing integration by parts [20] and using the identity $\partial G(K)/\partial \mathbf{k} = -G^2(K)\partial G^{-1}(K)/\partial \mathbf{k}$ then yields the following expression for $\overleftrightarrow{P}(0)$:

$$\overleftrightarrow{P}(0) = 2\sum_K G^2(K)\left\{\frac{\partial \xi_{\mathbf{k}}}{\partial \mathbf{k}} + \frac{\partial \Sigma_{pg}(K)}{\partial \mathbf{k}}\right\}\frac{\partial \xi_{\mathbf{k}}}{\partial \mathbf{k}}. \quad (2)$$

Here $K = (\omega, \mathbf{k})$. Given the self energy from Eq. (1), it is then straightforward to arrive at the quantity $\overleftrightarrow{P}(0)$:

$$\begin{aligned}\overleftrightarrow{P}(0) = 2\sum_K G^2(K)\Big\{&\frac{\partial \xi_{\mathbf{k}}}{\partial \mathbf{k}} - \Delta_1^2 G_{1,1}^2(-K)\frac{\partial \xi_{\mathbf{k},2}}{\partial \mathbf{k}} \\ &+ \Delta_1^2\Delta_2^2 G_{1,1}^2(-K)G_{0,4}^2(K)\frac{\partial \xi_{\mathbf{k},4}}{\partial \mathbf{k}} - \Delta_2^2 G_{1,2}^2(-K)\frac{\partial \xi_{\mathbf{k},1}}{\partial \mathbf{k}} \\ &+ \Delta_2^2\Delta_1^2 G_{1,2}^2(-K)G_{0,3}^2(K)\frac{\partial \xi_{\mathbf{k},3}}{\partial \mathbf{k}}\Big\}\frac{\partial \xi_{\mathbf{k}}}{\partial \mathbf{k}}. \quad (3)\end{aligned}$$

For simplicity, throughout the main text we set $C_1 = C_2 = 0$ and present the complete expressions in the supplement. Here we have defined the following four bare (inverse) Green's functions $G_{0,i}^{-1}(K) = (\omega - \xi_{\mathbf{k},i})$, $i \in \{1,2,3,4\}$, where $\xi_{\mathbf{k},1} = \xi_{\mathbf{k}+\mathbf{p}}$, $\xi_{\mathbf{k},2} = \xi_{\mathbf{k}-\mathbf{p}}$, $\xi_{\mathbf{k},3} = \xi_{\mathbf{k}+2\mathbf{p}}$, $\xi_{\mathbf{k},4} = \xi_{\mathbf{k}-2\mathbf{p}}$ are four dispersion relations. (The usual bare inverse Green's function is denoted by $G_0^{-1}(K) = \omega - \xi_{\mathbf{k}} = \omega - \epsilon_{\mathbf{k}} + \mu$.) The intermediate level Green's functions (which are neither bare nor full) associated with Eq. (1) are

$$G_{1,1}^{-1}(K) = \omega - \xi_{\mathbf{k},1} - \frac{\Delta_2^2}{\omega + \xi_{-\mathbf{k},4}}, \quad (4)$$

$$G_{1,2}^{-1}(K) = \omega - \xi_{\mathbf{k},2} - \frac{\Delta_1^2}{\omega + \xi_{-\mathbf{k},3}}. \quad (5)$$

In terms of these intermediate level Green's functions the self energy in Eq. (1) for the case where $C_1 = C_2 = 0$ has the compact form $\Sigma_{pg}(K) = -\Delta_1^2 G_{1,1}(-K) - \Delta_2^2 G_{1,2}(-K)$. The quantity $\overleftrightarrow{P}(0)$ in Eq. (3) provides a template for the form of the Feynman diagrams that we will find in $\overleftrightarrow{P}(Q)$.

Ward-Takahashi identity (WTI) for the full vertex.– The exact expression for the current-current correlation function, $\overleftrightarrow{P}(Q)$, is contained in the response functions written as

$$\begin{aligned}P^{\mu\nu}(Q) = 2\sum_K &\Gamma^\mu(K+Q,K)G(K) \\ &\times\gamma^\nu(K,K+Q)G(K+Q). \quad (6)\end{aligned}$$

The full vertex in four-vector notation is given by $\Gamma^\mu(K+Q,K) = (\Gamma^0(K+Q,K), \mathbf{\Gamma}(K+Q,K))$, where the first argument denotes the incoming momentum and the second argument, the outgoing momentum. Here the quantity $\gamma^\nu(K,K+Q)$ represents the bare vertex.

The full response kernel is $K^{\mu\nu}(Q) \equiv P^{\mu\nu}(Q) + \left(\frac{n}{m}\right)^{\mu\nu}_{\rm dia}(1 - \delta_{0,\nu}\delta_{\mu,\nu})$, where there is no summation over indices in the second term. The Ward-Takahashi identity in quantum field theory is a diagrammatic identity that imposes a symmetry between response functions. The particular symmetry we are interested in is the $\mathrm{U(1)_{EM}}$ abelian gauge symmetry [15]. Charge conservation is an exact relation between the current-current and density-density response functions that follows from this symmetry. As we shall show, satisfying the WTI also leads to manifestly sum rule consistent response functions.

The WTI is related to charge conservation which imposes the constraint: $\Omega K^{0\nu} + i\mathrm{div}_{\mathbf{q}} K^{j\nu} = 0$. The WTI for the vertex $\Gamma^\mu(K+Q,K)$ on a lattice is

$$\begin{aligned}&\Omega\Gamma^0(K+Q,K) + i\mathrm{div}_{\mathbf{q}}\mathbf{\Gamma}(K+Q,K) \\ &= G^{-1}(K+Q) - G^{-1}(K), \\ &= \Omega\gamma^0(K+Q,K) + i\mathrm{div}_{\mathbf{q}}\boldsymbol{\gamma}(K+Q,K) \\ &+ \Sigma_{pg}(K) - \Sigma_{pg}(K+Q). \quad (7)\end{aligned}$$

The WTI for the bare vertex $\gamma^\mu(K+Q,K)$ is $\Omega + i\mathrm{div}_{\mathbf{q}}\boldsymbol{\gamma} = G_0^{-1}(K+Q) - G_0^{-1}(K) = \Omega - \xi_{\mathbf{k}+\mathbf{q}} + \xi_{\mathbf{k}}$. Similarly we introduce the bare vertices $\gamma_i^\mu(K+Q,K)$ associated with the dispersions $\xi_{\mathbf{k},i}$. Here $\mathrm{div}_{\mathbf{q}}\mathbf{\Gamma}(K+Q,K)$, complicated by lattice effects, is the Fourier transform of the divergence of $\mathbf{\Gamma}$.

In the limit $Q \to 0$, the Ward-Takahashi identity reduces to the Ward identity: $\delta\Gamma^\mu(K,K) \equiv \Gamma^\mu(K,K) - \gamma^\mu(K,K) = -\partial\Sigma_{pg}(K)/\partial k_\mu$. This is fully consistent with the arguments leading up to the no-Meissner constraint in Eq. (2). In this continuum limit, ($q \to 0$) the WTI and charge conservation have familiar forms: $q_\mu\Gamma^\mu(K+Q,K) = G^{-1}(K+Q) - G^{-1}(K)$ and $q_\mu K^{\mu\nu}(Q) = 0$.

We emphasize that solving the WTI analytically for the full vertex $\Gamma^\mu(K+Q,K)$ is generally not possible, given an arbitrary self energy. However, there is a well-defined procedure to determine this vertex in principle. One inserts the bare vertex in all possible places in the self energy diagrams and sums the resulting series of diagrams. In the general case, where the self energy depends on the full Green's function, the series can be recast in the form of a Bethe-Salpeter equation [16].

The unique feature of BCS-based mean field approaches (and this applies to the inclusion of mean field spin and charge density wave effects as well [17]) is that the self energy can be expressed in terms of either a bare Green's function, or an intermediate level Green's function. This ensures that only finitely many bare vertex insertions are required. The full vertex can thus be deduced from the equivalent WTI by considering only finitely many loop diagrams.

We use the self energy of Eq. (1) to extract the full vertex $\Gamma^u(K+Q,K)$ via the WTI; this is inserted into Eq. (6) to yield

$$P^{\mu\nu}(Q) = 2\sum_K G(K)G(K+Q)\Big\{\gamma^\mu(K+Q,K)$$
$$+\Delta_1^2 G_{1,1}(-K)G_{1,1}(-K-Q)\left[\gamma_1^\mu(-K,-K-Q)+\Delta_2^2 G_{0,4}(K)G_{0,4}(K+Q)\gamma_4^\mu(K+Q,K)\right]$$
$$+\Delta_2^2 G_{1,2}(-K)G_{1,2}(-K-Q)\left[\gamma_2^\mu(-K,-K-Q)+\Delta_1^2 G_{0,3}(K)G_{0,3}(K+Q)\gamma_3^\mu(K+Q,K)\right]\Big\}\gamma^\nu(K,K+Q), \quad (8)$$

where the quantity in curly brackets is the full vertex function $\Gamma^\mu(K+Q,K)$. The Amperean pairing response functions would have nine associated Feynman diagrams if one considered the charge density wave: one of one loop order (two Green's functions), four of two loop order (four Green's functions), and four of three loop order (six Green's functions). The nine Feynman diagrams contributing to the response functions are presented in the Supplement.

The bare vertices for the density component are given by $\gamma^0(K+Q,K) = \gamma_i^0(K+Q,K) = 1$. This then allows the exact density-density response function $P_{\rho\rho}(Q)$ to be computed for all Q. More complicated, for an arbitrary band-structure, are the bare vertices that enter into the current-current correlation function. However, in the limit $q \to 0$ these can be determined from Eq. (3). The same reasoning which is used to determine $P_{\rho\rho}(Q)$ for all Q is applicable to the spin (density) response, as measured in neutron experiments.

The full spin response function $P_S^{\mu\nu}(Q)$ is defined by

$$P_S^{\mu\nu}(Q) = \sum_K \sum_\sigma \Gamma_{S_\sigma}^\mu(K+Q,K)G(K)$$
$$\times\gamma_{S_\sigma}^\nu(K,K+Q)G(K+Q). \quad (9)$$

Here the bare spin vertex is denoted by $\gamma_{S_\sigma}^\mu(K+Q,K)$, where $S_\sigma = \pm 1$ and $S_{\bar\sigma} = -S_\sigma$. The bare WTI for the spin vertex is $\Omega + i\mathrm{div}_{\mathbf{q}}\boldsymbol{\gamma}_{S_\sigma} = S_\sigma(G_0^{-1}(K+Q) - G_0^{-1}(K)) = S_\sigma(\Omega - \xi_{\mathbf{k}+\mathbf{q}} + \xi_{\mathbf{k}})$. Similarly the full WTI for the full spin vertex $\Gamma_{S_\sigma}^\mu(K+Q,K)$ is

$$\Omega\Gamma_{S_\sigma}^0 + i\mathrm{div}_{\mathbf{q}}\boldsymbol{\Gamma}_{S_\sigma} = S_\sigma(G^{-1}(K+Q) - G^{-1}(K)). \quad (10)$$

We can then read off the spin-spin correlation function directly using Eq. (8).

From the established constraints on the bare and full vertices one can directly derive [21] the f-sum rule for the density-density and spin density response functions:

$$\int \frac{d\omega}{\pi}(-\omega \mathrm{Im}P^{00}(Q)) = 2\sum_{\mathbf{k}} n_{\mathbf{k}}[\xi_{\mathbf{k}+\mathbf{q}} + \xi_{\mathbf{k}-\mathbf{q}} - 2\xi_{\mathbf{k}}], \quad (11)$$

where $n_{\mathbf{k}} = T\sum_{i\omega} G(K)$. Importantly, this sum rule (and counterparts for the current-current correlation function) are satisfied exactly providing the response functions are consistent with the Ward-Takahashi identity. This is discussed in more detail in the Supplement.

Behavior of the neutron cross section: Comparison of Pseudogap theories.– For illustrative purposes we focus on the spin-density response function, conventionally called $\chi_0(Q)$. Importantly, ensuring Eq. (11) is satisfied provides tight control over numerical calculations of this correlation function. When no simplifications are introduced, our numerical calculations agree with the sum rule to an accuracy of the order of $0.1-0.2$ percent [20] in all three models. The quantity $\mathrm{Im}\chi_0(Q) \equiv -\mathrm{Im}P^{00}(Q)$ in Eq. (8) is the theoretical basis for neutron scattering experiments. [Note we adopt the sign convention for the density correlation functions, $P_{\rho\rho}(Q) = P^{00}(Q)$ for spin and charge.]

For simple d-wave pairing models, a very reasonable comparison between theory and neutron data has been reported at high temperatures (where one sees a reflection of the fermiology [22, 23]) and below T_C (where one sees both commensurate (π,π) [24] and slightly incommensurate frequency dependent "hourglass" structure [25, 26]); this approach to neutron scattering presents a (rather successful) rival scheme to stripe approaches; many different theories, built on different microscopics, have arrived at similar behavior [27–30]. In the pseudogap phase (which has received less attention theoretically), there are peaks at and near (π,π) [4, 12, 13] which have been recently argued [4] to reflect some degree of broken orientational symmetry.

Here we compare the results for $\chi_0(Q)$ using three different theories of the pseudogap: a simple d-wave pseudogap, the theory of Yang, Rice and Zhang and that of Amperean pairing. For the latter we consider the reduced [6] 3×3 version (with $C_1 = C_2 = 0$ and dropping terms containing $\xi_{\mathbf{k}\pm 2\mathbf{p}}$). We do not include the effects of the widely used RPA enhanced denominator introduced in [31]. This will lead to a violation of the f-sum rule, and is not central to distinguishing between theories.

Figure (1) presents a plot of $\mathrm{Im}\chi^0(Q)$, for three fixed $\mathbf{q}$ corresponding to (π,π) in (a), $(\pi, 0.75\pi)$ in (b) and $(\pi,0)$ in (c) as functions of ω. The normal state (above T^*) band-structure is taken to be the same, as is the pseudogap amplitude. The behavior in the low ω regime is principally, but not exclusively, dominated by the effects of the gap, while at very high ω the behavior is band-structure dominated. Importantly, all theories essentially converge once ω is much larger than the gap.

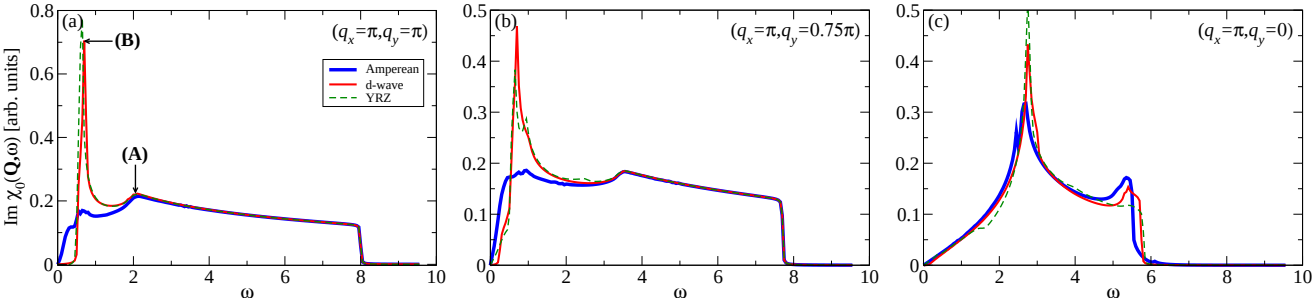

Figure 1. Comparison of the spin density correlation function $\mathrm{Im}\chi^0(Q) = -\mathrm{Im}P_S^{00}(\mathbf{q},\omega)$ for three different values of $\mathbf{q}$ in the Amperean, d-wave and YRZ pseudogap theories. In (a) we have labeled the Van Hove peaks appearing in the d-wave theory, which appear as saddle points in the contour plot of Fig. (2). Here we use the band structure given in [3] with $T = 0.01$ and a broadening of $\Gamma = 0.01$. The doping $p = 0.12$ and the chemical potential μ is fixed by the Luttinger sum rule. The band-structure and frequency are all normalized by t, and the gap function has an amplitude of $\Delta_0 = 0.15$. For the Amperean theory we use a k_x, k_y-symmetrized Gaussian [6] gap function.

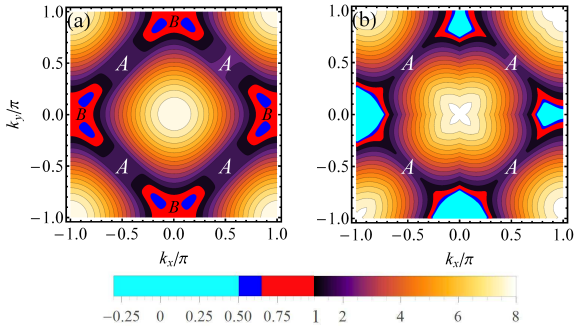

Figure 2. The equal energy contours $E_2(\mathbf{k}) \equiv E_{\mathbf{k}} + E_{\mathbf{k}+\mathbf{q}}$ which appear as the integrand in $\mathrm{Im}\chi^0(\mathbf{q},\omega)$ for both (a) d-wave and (b) the Amperean pseudogap schemes. Here $\mathbf{q} = (\pi,\pi)$. Note there are several energy scales as indicated by the legend. The labels A and B indicate the location of the saddle points of $\mathrm{Im}\chi^0(\mathbf{q},\omega)$.

This means that unusual and very interesting effects associated with high energy scales [14] such as observed in recent RIXS experiments, would not be specific to a given theory.

Figure (1) shows that there is little difference in the spin dynamics between the approach of YRZ [7] and that of a d-wave pseudogap, emphasized earlier in a different context [32] and helps to explain the literature claims of successful reconciliation with the data that surround both scenarios [25, 26, 30].

What appears most distinctive is the Amperean pairing theory, particularly away from $\mathbf{q} = (\pi, 0)$. Notable here is the absence of the sharp Van Hove peak (marked by B in Fig. (1)) which appears in both other theories and which is ultimately responsible for commensurate peaks or neutron resonance effects [24]. Also missing from the Amperean scenario is the so-called spin-gap, apparent at (π,π) in both the other two theories. Rather, for Amperean pairing there are multiple low energy processes which contribute to the spin density correlation function.

To better understand these processes, in Fig. (2) we probe the dominant component of the integrand in $\mathrm{Im}\chi^0(Q)$ near $\mathbf{q} = (\pi,\pi)$ for the Amperean (right) as compared with d-wave pseudogap (left) scenarios. We show the equal energy contours for the sum of the quasiparticle dispersions: $E_2(\mathbf{k}) \equiv E_{\mathbf{k}} + E_{\mathbf{k}+\mathbf{q}}$, vs k_x and k_y in the pseudogap state [33]. Indicated on the figure are the Van Hove singularities A and B (saddle points in the contour plot), as labeled in Figure (1a). The lower energy Van Hove point (point B) is clearly suppressed in the Amperean pairing case, while it is very pronounced and found to be quite important [26] for the d-wave case. Also evident from the cyan region in Fig. (2) is the absence of a low ω minimum (spin gap) in $E_2(\mathbf{k})$, as found in both the other two theories, as well as in the integrated response function.

Conclusions.– The central contribution of this paper has been to establish an analytically and numerically controlled methodology for addressing the long list of two particle cuprate measurements. Given a mean field like self energy, the exploitation of the Ward Takahashi identity (and related sum rules) allows one to evaluate two particle properties, and in this way achieve the same level of accuracy in these comparisons, as in, say, ARPES. To demonstrate the utility of this method, we address the spin density response functions of neutron scattering and have singled out signatures of the recently proposed Amperean pairing theory [6]. We cannot firmly establish that this pair density wave theory is inconsistent with experiments (without digressing from our goals and including the sum-rule-inconsistent RPA enhancement denominator [31]), but it does lead to a rather featureless neutron cross section [34]. We report two distinctive observations: the absence of both spin gap effects and of the sharp Van Hove peaks near (π,π).

This work is supported by NSF-MRSEC Grant 0820054. We are grateful to A.-M. S. Tremblay, Yan He and A. Rançon for helpful conversations.

[1] G. Ghiringhelli *et al*, Science **337**, 821 (2012).
[2] W. D. Wise, M. C. Boyer, K. Chatterjee, T. Kondo, T. Takeuchi, H. Ikuta, Y. Wang, and E. W. Hudson, Nature Physics **4**, 696 (2008).
[3] R. Comin *et al*, Science **343**, 390 (2014).
[4] V. Hinkov, P. Bourges, S. Pailhès, Y. Sidis, A. Ivanov, C. D. Frost, T. G. Perring, C. T. Lin, D. P. Chen, and B. Keimer, Nature Physics **3**, 780 (2007).
[5] H.-D. Chen, O. Vafek, A. Yazdani, and S.-C. Zhang, Phys. Rev. Lett. **93**, 187002 (2004).
[6] P. A. Lee, Phys. Rev. X **4**, 031017 (2014).
[7] K.-Y. Yang, T. M. Rice, and F.-C. Zhang, Phys. Rev. B **73**, 174501 (2006).
[8] A. Damascelli, Z. Hussain, and Z.-X. Shen, Rev. Mod. Phys. **75**, 473 (2003).
[9] J. Corson, R. Mallozzi, J. Orenstein, J. N. Eckstein, and I. Bozovic, Nature **398**, 221 (1999).
[10] L. Li, Y. Wang, S. Komiya, S. Ono, Y. Ando, G. D. Gu, and N. P. Ong, Phys. Rev. B **81**, 054510 (2010).
[11] S. H. Pan, E. W. Hudson, A. K. Gupta, K.-W. Ng, H. Eisaki, S. Uchida, and J. C. Davis, Phys. Rev. Lett. **85**, 1536 (2000).
[12] C. Stock, W. J. L. Buyers, R. Liang, D. Peets, Z. Tun, D. Bonn, W. N. Hardy, and R. J. Birgeneau, Phys. Rev. B **69**, 014502 (2004).
[13] P. Dai, H. A. Mook, S. M. Hayden, G. Aeppli, T. G. Perring, R. D. Hunt, and F. Doğan, Science **284**, 1344 (1999).
[14] M. L. Tacon *et al*, Nature Physics **7**, 725 (2011).
[15] L. H. Ryder, *Quantum Field Theory* (Cambridge University Press, 1996), 2nd ed.
[16] J. R. Schrieffer, *Theory of Superconductivity* (W.A. Benjamin, Inc., 1964), 1st ed.
[17] D. Podolsky, E. Demler, K. Damle, and B. I. Halperin, Phys. Rev. B **67**, 094514 (2004).
[18] Q. J. Chen, J. Stajic, S. N. Tan, and K. Levin, Phys. Rep. **412**, 1 (2005).
[19] M. R. Norman, M. Randeria, H. Ding, and J. C. Campuzano, Phys. Rev. B **57**, 11093(R) (1998).
[20] For simplicity in the text, we will ignore terms that arise from the wave vector dependence of the d-wave gap function. In general this is a small effect. We can see via the sum rule accuracy the importance of including the full wave vector dependence of the d-wave gap. When the wave vector dependence of the gap is ignored, the sum rule accuracy is still very good, but now of the order of 2-3 percent.
[21] D. Bergeron, D. Hankevych, B. Kyung, and A.-M. S. Tremblay, Phys. Rev. B **84**, 085128 (2011).
[22] Q. Si, Y. Zha, K. Levin, and J. P. Lu, Phys. Rev. B **47**, 9055 (1993).
[23] Y. Zha, Q. Si, and K. Levin, Physica C **212**, 413 (1993).
[24] D. Z. Liu, Y. Zha, and K. Levin, Phys. Rev. Lett. **75**, 4130 (1995).
[25] Y. Zha, K. Levin, and Q. Si, Phys. Rev. B **47**, 9124 (1993).
[26] Y.-J. Kao, Q. M. Si, and K. Levin, Phys. Rev. B **61**, R118980 (2000).
[27] G. Stemmann, C. Pépin, and M. Lavagna, Phys. Rev. B **50**, 4075 (1994).
[28] J. Brinckmann and P. A. Lee, Phys. Rev. Lett. **82**, 2915 (1999).
[29] M. R. Norman, Phys. Rev. B **61**, 14751 (2000).
[30] A. J. A. James, R. M. Konik, and T. M. Rice, Phys. Rev. B **86**, 100508(R) (2012).
[31] Q. Si, J. P. Lu, and K. Levin, Phys. Rev. B. **45**, 4930 (1992).
[32] P. Scherpelz, A. Rançon, Y. He, and K. Levin, Phys. Rev. B **90**, 060506(R) (2014).
[33] For the 3×3 Amperean theory, we chose the top band for both $E_{\mathbf{k}}$ and $E_{\mathbf{k+q}}$.
[34] In addition to the gaussian gap model of Ref. [6], we have found similar featureless results for a simple d-wave gap shape as well.

Supplementary material

I. INCLUSION OF BOTH CHARGE DENSITY WAVE AND PAIR DENSITY WAVE EFFECTS

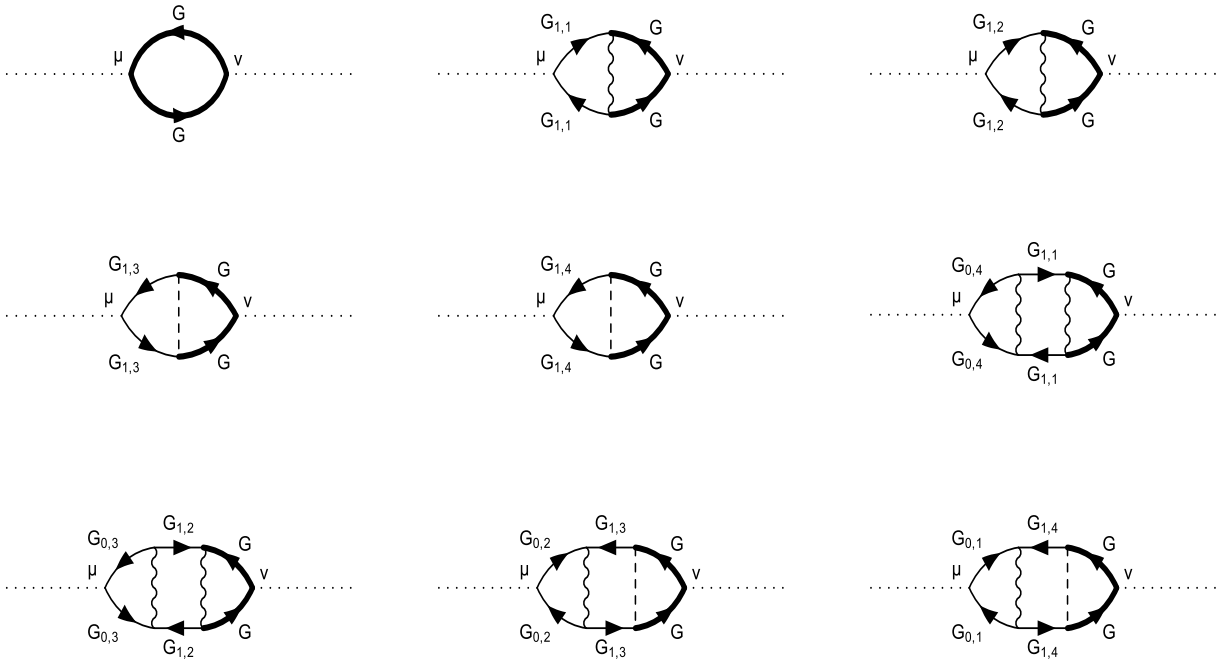

Figure 1. All nine Feynman diagrams which contribute to the response functions $P^{\mu\nu}(Q)$.

In this supplement we extend our results to include the effects of the pair densities C_1 and C_2: $C_1, C_2 \neq 0$. This requires another two intermediate level Green's functions in addition to the two in Eqs. (4-5) of the main text:

$$G_{1,3}^{-1}(K) = \omega - \xi_{\mathbf{k},3} - \frac{\Delta_1^2}{\omega + \xi_{\mathbf{k},1}}, \tag{1}$$

$$G_{1,4}^{-1}(K) = \omega - \xi_{\mathbf{k},4} - \frac{\Delta_2^2}{\omega + \xi_{\mathbf{k},2}}. \tag{2}$$

The full self energy of the Amperean pairing theory is then $\Sigma_{pg}(K) = -\Delta_1^2 G_{1,1}(-K) - \Delta_2^2 G_{1,2}(-K) + C_1^2 G_{1,3}(K) + C_2^2 G_{1,4}(K)$. Since the full self energy contains only intermediate level Green's functions, the Ward-Takahashi identity (WTI) allows the full vertex $\Gamma^\mu(K+Q, K)$ to be obtained explicitly. Using the full vertex obtained from the WTI, the response functions are then

$$\begin{aligned}
P^{\mu\nu}(Q) = 2\sum_K G(K)G(K+Q)\Big\{ & \gamma^\mu(K+Q,K) \\
& + \Delta_1^2 G_{1,1}(-K)G_{1,1}(-K-Q)\left[\gamma_1^\mu(-K,-K-Q) + \Delta_2^2 G_{0,4}(K)G_{0,4}(K+Q)\gamma_4^\mu(K+Q,K)\right] \\
& + C_1^2 G_{1,3}(K)G_{1,3}(K+Q)\left[\gamma_3^\mu(K+Q,K) + \Delta_1^2 G_{0,2}(-K)G_{0,2}(-K-Q)\gamma_2^\mu(-K,-K-Q)\right] \\
& + \Delta_2^2 G_{1,2}(-K)G_{1,2}(-K-Q)\left[\gamma_2^\mu(-K,-K-Q) + \Delta_1^2 G_{0,3}(K)G_{0,3}(K+Q)\gamma_3^\mu(K+Q,K)\right] \\
& + C_2^2 G_{1,4}(K)G_{1,4}(K+Q)\left[\gamma_4^\mu(K+Q,K) + \Delta_2^2 G_{0,1}(-K)G_{0,1}(-K-Q)\gamma_1^\mu(-K,-K-Q)\right]\Big\}\gamma^\nu(K,K+Q),
\end{aligned} \tag{3}$$

where the quantity in the curly brackets is the full vertex function [1]. There are nine Feynman diagrams that contribute to the response functions, which are shown in Figure (1). In the more general case of wave vector dependent gaps, there are additional terms involving the derivatives of the gap, which, in the 3×3 matrix representation theory give an essentially negligible contribution.

The response functions are completely specified once the various bare vertices are given. We have to rely on the semi-classical approximation to obtain the form of the bare vertices associated with the current. In the limit $\mathbf{q} \to 0$, this approximation becomes rigorously correct.

II. RELATION BETWEEN SUM RULES AND THE WARD-TAKAHASHI IDENTITY

A. f-sum rule

The exact response functions are given in Eq. (3). (We take the density-density correlation function to be $P_{\rho\rho}(Q) = P^{00}(Q)$ and the current-current correlation function is $\overleftrightarrow{P}(Q) = P^{ij}(Q)$, $i, j \in \{1, 2, 3\}$.) In the main text we assert that, given bare and full vertices that satisfy the associated WTI, the following f-sum rule is satisfied

$$\int \frac{d\omega}{\pi}(-\omega \mathrm{Im}P^{00}(Q)) = 2\sum_{\mathbf{k}} n_{\mathbf{k}}(\xi_{\mathbf{k}+\mathbf{q}} + \xi_{\mathbf{k}-\mathbf{q}} - 2\xi_{\mathbf{k}}), \tag{4}$$

where $n_{\mathbf{k}} = T\sum_{i\omega} G(K)$. This sum rule can be established as follows.

The WTI for the full and bare vertices [2], $\Gamma^{\mu}(K+Q, K) = (\Gamma^0(K+Q, K), \mathbf{\Gamma}(K+Q, K))$ and $\gamma^{\mu}(K+Q, K) = (1, \boldsymbol{\gamma}(K+Q, K))$ are

$$\begin{aligned} \Omega\Gamma^0 + i\mathrm{div}_{\mathbf{q}}\mathbf{\Gamma} &= G^{-1}(K+Q) - G^{-1}(K), \\ \Omega + i\mathrm{div}_{\mathbf{q}}\boldsymbol{\gamma} &= G_0^{-1}(K+Q) - G_0^{-1}(K) = \Omega - \xi_{\mathbf{k}+\mathbf{q}} + \xi_{\mathbf{k}}. \end{aligned} \tag{5}$$

The response kernel is defined as $K^{\mu\nu}(Q) = P^{\mu\nu}(Q) + \left(\frac{n}{m}\right)^{\mu\nu}_{\mathrm{dia}}(1 - \delta_{0,\nu}\delta_{\mu,\nu})$, where there is no summation over indices in the second term. Applying the WTI to $K^{\mu 0}$ while setting $\nu = 0$ the result is

$$\Omega P^{00} + i\mathrm{div}_{\mathbf{q}}P^{i0} = 2\sum_{K} G(K+Q)G(K)[G^{-1}(K+Q) - G^{-1}(K)] = 0. \tag{6}$$

If we set $\nu = j = \{1, 2, 3\}$ and apply the WTI to $K^{\mu j}$ the result is

$$\Omega P^{0j} + i\mathrm{div}_{\mathbf{q}}P^{ij} = 2\sum_{K} G(K)[\boldsymbol{\gamma}(K, K+Q) - \boldsymbol{\gamma}(K-Q, K)]. \tag{7}$$

Setting $\Omega = 0$ and then operating with $i\mathrm{div}_{\mathbf{q}}$ gives

$$i\mathrm{div}_{\mathbf{q}}i\mathrm{div}_{\mathbf{q}}P^{ij}(\mathbf{q}, 0) = 2\sum_{\mathbf{k}} n_{\mathbf{k}}[2\xi_{\mathbf{k}} - \xi_{\mathbf{k}+\mathbf{q}} - \xi_{\mathbf{k}-\mathbf{q}}]. \tag{8}$$

Now use the identity $\mathrm{Im}P^{i0}(\mathbf{q}, \omega) = -\mathrm{Im}P^{0i}(-\mathbf{q}, -\omega)$ and Eq. (6), Eq. (7) and Eq. (8) to solve for $\mathrm{Im}P^{00}$ in terms of $\mathrm{Im}P^{ij}$. By applying the Kramers-Kronig relations we then have the sum rule in Eq. (4). Importantly, we have proved the f-sum rule for all values of $\mathbf{q}$. This proof depends on having bare and full vertices $\gamma^{\mu}(K+Q, K)$ and $\Gamma^{\mu}(K+Q, K)$ which satisfy the Ward Takahashi identity.

B. Longitudinal sum rule

By using the relationship between $\mathrm{Im}P^{ij}$ and $\mathrm{Im}P^{00}$, along with the f-sum rule, the longitudinal sum rule is obtained. The abstract form of the longitudinal sum rule is

$$\int \frac{d\omega}{\pi}\left(-\frac{\mathrm{Im}\{i\mathrm{div}_{\mathbf{q}}i\mathrm{div}_{\mathbf{q}}\overleftrightarrow{P}(Q)\}}{\omega}\right) = 2\sum_{\mathbf{k}} n_{\mathbf{k}}(\xi_{\mathbf{k}+\mathbf{q}} + \xi_{\mathbf{k}-\mathbf{q}} - 2\xi_{\mathbf{k}}). \tag{9}$$

The WTI for the bare vertices implies that $i\mathrm{div}_{\mathbf{q}}\gamma = \xi_{\mathbf{k}} - \xi_{\mathbf{k}+\mathbf{q}}$. Thus by applying this identity to the vertices that appear in Eq. (3), the longitudinal sum rule is manifestly satisfied. While the response functions can be shown to satisfy the longitudinal sum rule based on the WTI, an explicit proof is somewhat more difficult. For free particle dispersion there is no difficulty. The complication is due to the fact that the bare vertex $\boldsymbol{\gamma}(K+Q, K)$ can be written down only in the small $\mathbf{q}$ limit in a periodic potential. Here one imposes the semi-classical approximation, appropriate to $\mathbf{q} \to 0$, so that the bare vertices are given by

$$\gamma^{\mu}_{i}(K+Q, K) = \frac{\partial \xi_{\mathbf{k}+\mathbf{q}/2,i}}{\partial \mathbf{k}}. \tag{10}$$

In the limit that $\mathbf{q} \to 0$ the current-current correlation function becomes

$$\begin{aligned}\overleftrightarrow{P}(Q) = 2\sum_K G(K)G(K+Q)\Big\{ & \frac{\partial \xi_{\mathbf{k}+\mathbf{q}/2}}{\partial \mathbf{k}} \\ & + \Delta_1^2 G_{1,1}(-K)G_{1,1}(-K-Q)\left[-\frac{\partial \xi_{\mathbf{k}+\mathbf{q}/2,2}}{\partial \mathbf{k}} + \Delta_2^2 G_{0,4}(K)G_{0,4}(K+Q)\frac{\partial \xi_{\mathbf{k}+\mathbf{q}/2,4}}{\partial \mathbf{k}}\right] \\ & + C_1^2 G_{1,3}(K)G_{1,3}(K+Q)\left[\frac{\partial \xi_{\mathbf{k}+\mathbf{q}/2,3}}{\partial \mathbf{k}} - \Delta_1^2 G_{0,2}(-K)G_{0,2}(-K-Q)\frac{\partial \xi_{\mathbf{k}+\mathbf{q}/2,1}}{\partial \mathbf{k}}\right] \\ & + \Delta_2^2 G_{1,2}(-K)G_{1,2}(-K-Q)\left[-\frac{\partial \xi_{\mathbf{k}+\mathbf{q}/2,1}}{\partial \mathbf{k}} + \Delta_1^2 G_{0,3}(K)G_{0,3}(K+Q)\frac{\partial \xi_{\mathbf{k}+\mathbf{q}/2,3}}{\partial \mathbf{k}}\right] \\ & + C_2^2 G_{1,4}(K)G_{1,4}(K+Q)\left[\frac{\partial \xi_{\mathbf{k}+\mathbf{q}/2,4}}{\partial \mathbf{k}} - \Delta_2^2 G_{0,1}(-K)G_{0,1}(-K-Q)\frac{\partial \xi_{\mathbf{k}+\mathbf{q}/2,2}}{\partial \mathbf{k}}\right]\Big\}\frac{\partial \xi_{\mathbf{k}+\mathbf{q}/2}}{\partial \mathbf{k}}, \end{aligned} \tag{11}$$

which is in agreement with the form of $\overleftrightarrow{P}(0)$ obtained in Eq. (3) of the main text by imposing the absence of a Meissner effect in the normal phase. The longitudinal sum rule in this particular limit reduces to

$$\int \frac{d\omega}{\pi}\left(-\frac{\mathrm{Im}\mathbf{q}\cdot\overleftrightarrow{P}(Q)\cdot\mathbf{q}}{\omega}\right) = 2\sum_{\mathbf{k}} n_{\mathbf{k}}(\xi_{\mathbf{k}+\mathbf{q}} + \xi_{\mathbf{k}-\mathbf{q}} - 2\xi_{\mathbf{k}}), \tag{12}$$

which is in agreement with Appendix A of [3].

C. Transverse sum rule

The longitudinal and f-sum rules are consequences of the WTI and the associated $\mathrm{U}(1)_{\mathrm{EM}}$ symmetry. The transverse sum rule is, however, unrelated to the WTI. Rather, it is a statement about the analyticity of the current-current correlation function. For completeness we verify the transverse sum rule for the current-current correlation function in the Amperean pairing theory.

For convenience we define the following Green's functions and bare vertices:

Table I. Definitions of Green's functions and bare vertices.

Green's functions		Bare vertices	
$\tilde{G}_0(K)$	$G(K)$	$\tilde{\gamma}_0^\mu(K+Q,K)$	$\gamma^\mu(K+Q,K)$
$\tilde{G}_1(K)$	$\Delta_1 G_{1,1}(-K)G(K)$	$\tilde{\gamma}_1^\mu(K+Q,K)$	$\gamma_1^\mu(-K,-K-Q)$
$\tilde{G}_2(K)$	$\Delta_2 G_{1,2}(-K)G(K)$	$\tilde{\gamma}_2^\mu(K+Q,K)$	$\gamma_2^\mu(-K,-K-Q)$
$\tilde{G}_3(K)$	$\Delta_2\Delta_1 G_{1,2}(-K)G_{0,3}(K)G(K)$	$\tilde{\gamma}_3^\mu(K+Q,K)$	$\gamma_3^\mu(K+Q,K)$
$\tilde{G}_4(K)$	$\Delta_1\Delta_2 G_{1,1}(-K)G_{0,4}(K)G(K)$	$\tilde{\gamma}_4^\mu(K+Q,K)$	$\gamma_4^\mu(K+Q,K)$
$\tilde{G}_5(K)$	$C_1 G_{1,3}(K)G(K)$	$\tilde{\gamma}_5^\mu(K+Q,K)$	$\gamma_3^\mu(K+Q,K)$
$\tilde{G}_6(K)$	$C_2 G_{1,4}(K)G(K)$	$\tilde{\gamma}_6^\mu(K+Q,K)$	$\gamma_4^\mu(K+Q,K)$
$\tilde{G}_7(K)$	$C_1\Delta_1 G_{1,3}(K)G_{0,2}(-K)G(K)$	$\tilde{\gamma}_7^\mu(K+Q,K)$	$\gamma_2^\mu(-K,-K-Q)$
$\tilde{G}_8(K)$	$C_2\Delta_2 G_{1,4}(K)G_{0,1}(-K)G(K)$	$\tilde{\gamma}_8^\mu(K+Q,K)$	$\gamma_1^\mu(-K,-K-Q)$

The current-current correlation function is then

$$\overleftrightarrow{P}(Q) = 2\sum_K\sum_{a=0}^{8}\tilde{\boldsymbol{\gamma}}_a(K+Q,K)\tilde{G}_a(K)\boldsymbol{\gamma}(K,K+Q)\tilde{G}_a(K+Q). \tag{13}$$

The transverse sum rule is given by the following Kramers-Kronig relation

$$\lim_{\mathbf{q}\to 0}\int\frac{d\omega}{\pi}\left(-\frac{\mathrm{Im}P_T(\mathbf{q},\omega)}{\omega}\right) = -P_T(0). \tag{14}$$

Here $P_T(Q)$ is the transverse part of the current-current correlation function: $P_T(Q) = (\sum_i P^{ii}(Q) - P_L(Q))/2$, where $P_L(Q) = \hat{\mathbf{q}}\cdot\overleftrightarrow{P}(Q)\cdot\hat{\mathbf{q}}$ is the longitudinal part of the current-current correlation function.

The Green's function $\tilde{G}_a(K)$ can be written as

$$\tilde{G}_a(K) = \sum_i \frac{R^i_{a,\mathbf{k}}}{i\omega - E^i_{a,\mathbf{k}}}, \tag{15}$$

where $E^i_{a,\mathbf{k}}$ is the ith pole of the Green's function $\tilde{G}_a(K)$ and $R^i_{a,\mathbf{k}}$ is the associated residue. The spectral representation of the Green's function $\tilde{G}_a(K)$ is

$$\tilde{G}_a(K) = \int \frac{dx}{2\pi} \frac{A_{a,\mathbf{k}}(x)}{i\omega - x}. \tag{16}$$

The spectral functions $A_{a,\mathbf{k}}(x)$ are explicitly given by

$$A_{a,\mathbf{k}}(x) = 2\pi \sum_i R^i_{a,\mathbf{k}} \delta(x - E^i_{a,\mathbf{k}}). \tag{17}$$

Using the spectral representation of the Green's functions, we have

$$\begin{aligned} T\sum_{i\omega}[\tilde{G}_a(K)]^2 &= T\sum_{i\omega}\int \frac{dx}{2\pi}\frac{dy}{2\pi}\frac{A_{a,\mathbf{k}}(x)}{i\omega - x}\frac{A_{a,\mathbf{k}}(y)}{i\omega - y}, \\ &= T\sum_{i\omega}\sum_{i,j}\int dxdy \frac{R^i_{a,\mathbf{k}}\delta(x - E^i_{a,\mathbf{k}})}{i\omega - x}\frac{R^j_{a,\mathbf{k}}\delta(y - E^j_{a,\mathbf{k}})}{i\omega - y}, \\ &= T\sum_{i\omega}\Bigg(\sum_{i\neq j}\frac{R^i_{a,\mathbf{k}}R^j_{a,\mathbf{k}}}{(i\omega - E^i_{a,\mathbf{k}})(i\omega - E^j_{a,\mathbf{k}})} + \sum_i \frac{(R^i_{a,\mathbf{k}})^2}{(i\omega - E^i_{a,\mathbf{k}})^2}\Bigg), \\ &= \sum_{i\neq j} R^i_{a,\mathbf{k}}R^j_{a,\mathbf{k}}\frac{f(E^i_{a,\mathbf{k}}) - f(E^j_{a,\mathbf{k}})}{E^i_{a,\mathbf{k}} - E^j_{a,\mathbf{k}}} + \sum_i (R^i_{a,\mathbf{k}})^2 f'(E^i_{a,\mathbf{k}}). \end{aligned} \tag{18}$$

The right hand side of the transverse sum rule is thus

$$\begin{aligned} -P_T(0) &= -2\sum_K\sum_{a=0}^{8}\tilde{\boldsymbol{\gamma}}^T_a(K,K)[\tilde{G}_a(K)]^2\boldsymbol{\gamma}^T(K,K) \\ &= -2\sum_{\mathbf{k}}\sum_{a=0}^{8}\tilde{\boldsymbol{\gamma}}^T_a(K,K)\Bigg(\sum_{i\neq j}R^i_{a,\mathbf{k}}R^j_{a,\mathbf{k}}\frac{f(E^i_{a,\mathbf{k}}) - f(E^j_{a,\mathbf{k}})}{E^i_{a,\mathbf{k}} - E^j_{a,\mathbf{k}}} + \sum_i (R^i_{a,\mathbf{k}})^2 f'(E^i_{a,\mathbf{k}})\Bigg)\boldsymbol{\gamma}^T(K,K). \end{aligned} \tag{19}$$

The left hand side of the transverse sum rule can be calculated as follows.

Using spectral representations we have

$$\begin{aligned} H(\mathbf{q}, i\Omega,) = T\sum_{i\omega}\tilde{G}_a(K)\tilde{G}_a(K+Q) &= T\sum_{i\omega}\int \frac{dx}{2\pi}\frac{dy}{2\pi}\frac{A_{a,\mathbf{k}}(x)}{i\omega - x}\frac{A_{a,\mathbf{k}+\mathbf{q}}(y)}{i\omega + i\Omega - y}, \\ &= \int \frac{dx}{2\pi}\frac{dy}{2\pi}A_{a,\mathbf{k}}(x)A_{a,\mathbf{k}+\mathbf{q}}(y)\Bigg(\frac{f(x) - f(y)}{x - y + i\Omega}\Bigg). \end{aligned} \tag{20}$$

It follows that, upon analytic continuation $i\Omega \to \omega + i0^+$, we have

$$\int \frac{d\omega}{\pi}\Bigg(-\frac{\mathrm{Im}H(\mathbf{q},\omega)}{\omega}\Bigg) = \int \frac{dx}{2\pi}\frac{dy}{2\pi}A_{a,\mathbf{k}}(x)A_{a,\mathbf{k}+\mathbf{q}}(y)\Bigg(\frac{f(x) - f(y)}{y - x}\Bigg). \tag{21}$$

Inserting the explicit form of the spectral functions then gives

$$\int \frac{d\omega}{\pi}\Bigg(-\frac{\mathrm{Im}H(\mathbf{q},\omega)}{\omega}\Bigg) = \sum_{i,j} R^i_{a,\mathbf{k}}R^j_{a,\mathbf{k}+\mathbf{q}}\frac{f(E^i_{a,\mathbf{k}}) - f(E^j_{a,\mathbf{k}+\mathbf{q}})}{E^j_{a,\mathbf{k}+\mathbf{q}} - E^i_{a,\mathbf{k}}}. \tag{22}$$

The limit $\mathbf{q}\to 0$ of $R^j_{a,\mathbf{k}+\mathbf{q}}$ is well defined, as is that of $\frac{f(E^i_{a,\mathbf{k}})-f(E^j_{a,\mathbf{k}+\mathbf{q}})}{E^j_{a,\mathbf{k}+\mathbf{q}}-E^i_{a,\mathbf{k}}}$, for $i\neq j$. (Similarly the bare vertices are well defined in this limit.) It follows that

$$-\lim_{\mathbf{q}\to 0}\int\frac{d\omega}{\pi}\left(-\frac{\mathrm{Im}H(\mathbf{q},\omega)}{\omega}\right)=\sum_{i\neq j}R^i_{a,\mathbf{k}}R^j_{a,\mathbf{k}}\frac{f(E^i_{a,\mathbf{k}})-f(E^j_{a,\mathbf{k}})}{E^i_{a,\mathbf{k}}-E^j_{a,\mathbf{k}}}+\sum_i(R^i_{a,\mathbf{k}})^2f'(E^i_{a,\mathbf{k}}). \tag{23}$$

Thus the left hand side of the transverse sum rule is

$$\begin{aligned}&\lim_{\mathbf{q}\to 0}\int\frac{d\omega}{\pi}\left(-\frac{\mathrm{Im}P_T(\mathbf{q},\omega)}{\omega}\right)\\&=-2\sum_{\mathbf{k}}\sum_{a=0}^{8}\tilde{\boldsymbol{\gamma}}^T_a(K,K)\left(\sum_{i\neq j}R^i_{a,\mathbf{k}}R^j_{a,\mathbf{k}}\frac{f(E^i_{a,\mathbf{k}})-f(E^j_{a,\mathbf{k}})}{E^i_{a,\mathbf{k}}-E^j_{a,\mathbf{k}}}+\sum_i(R^i_{a,\mathbf{k}})^2f'(E^i_{a,\mathbf{k}})\right)\boldsymbol{\gamma}^T(K,K).\end{aligned} \tag{24}$$

This is equivalent to Eq. (19), which is the right hand side of the transverse sum rule.

III. SPIN RESPONSE FUNCTIONS

In this section we extend our results to include spin response functions. Let $\sigma=\uparrow\downarrow$ denote spin indices with $\overline{\sigma}$ the opposite of σ. The density-density and current-current correlation functions are response functions related by the $\mathrm{U(1)_{EM}}$ gauge symmetry and the associated Ward-Takahashi identity. The analogous spin response functions are related by the $\mathrm{U(1)_z}$ gauge symmetry and the associated Ward-Takahashi identity.

The familiar $\mathrm{U(1)_{EM}}$ gauge theory is based on the four-vector potential $A^\mu=(\phi,\mathbf{A})$. For the $\mathrm{U(1)_z}$ gauge theory the external vector field is $A^\mu=(B_z,\mathbf{m})$, where $\mathbf{m}$ is the magnetization. The associated Hamiltonian describes a generalized spin-magnetic field interaction, and the Noether current for the global $\mathrm{U(1)_z}$ symmetry is a magnetization current. An important difference between these two symmetries is that below T_C the $\mathrm{U(1)_{EM}}$ gauge symmetry is spontaneously broken. Thus to restore gauge invariance collective mode effects must be incorporated. On the other hand the $\mathrm{U(1)_z}$ gauge symmetry is not spontaneously broken and therefore does not require any collective physics. Since we are only considering the response functions above T_C this difference is not central to our discussion.

The bare spin vertex is denoted by $\gamma^\mu_{S_\sigma}(K+Q,K)$, where $S_\sigma=\pm 1$ and $S_{\bar\sigma}=-S_\sigma$ The bare and full Ward-Takahashi identities for the spin vertices are discussed in the main text [see Eq. (10) of the main text].

The full spin response function $P^{\mu\nu}_S(Q)$ is defined by

$$P^{\mu\nu}_S(Q)=\sum_K\sum_\sigma G(K+Q)\Gamma^\mu_{S_\sigma}(K+Q,K)G(K)\gamma^\nu_{S_\sigma}(K,K+Q). \tag{25}$$

Following the main text, given the form of the self energy the WTI can be used to extract the full vertex, for both the charge and spin response functions. Explicitly, the exact spin response functions are

$$\begin{aligned}P^{\mu\nu}_S(Q)=&\sum_\sigma\sum_K G(K)G(K+Q)\Big\{\gamma^\mu_{S_\sigma}(K+Q,K)\\&+\Delta_1^2G_{1,1}(-K)G_{1,1}(-K-Q)\left[\gamma^\mu_{1,S_\sigma}(-K,-K-Q)+\Delta_2^2G_{0,4}(K)G_{0,4}(K+Q)\gamma^\mu_{4,S_\sigma}(K+Q,K)\right]\\&+C_1^2G_{1,3}(K)G_{1,3}(K+Q)\left[\gamma^\mu_{3,S_\sigma}(K+Q,K)+\Delta_1^2G_{0,2}(-K)G_{0,2}(-K-Q)\gamma^\mu_{2,S_\sigma}(-K,-K-Q)\right]\\&+\Delta_2^2G_{1,2}(-K)G_{1,2}(-K-Q)\left[\gamma^\mu_{2,S_\sigma}(-K,-K-Q)+\Delta_1^2G_{0,3}(K)G_{0,3}(K+Q)\gamma^\mu_{3,S_\sigma}(K+Q,K)\right]\\&+C_2^2G_{1,4}(K)G_{1,4}(K+Q)\left[\gamma^\mu_{4,S_\sigma}(K+Q,K)+\Delta_2^2G_{0,1}(-K)G_{0,1}(-K-Q)\gamma^\mu_{1,S_\sigma}(-K,-K-Q)\right]\Big\}\gamma^\nu_{S_\sigma}(K,K+Q),\end{aligned} \tag{26}$$

The proof of the f-sum rule in section (II. A) can be performed for the spin response function $P^{00}_S(Q)$ in an analogous manner, by using the WTI for the spin vertices. In this case we obtain

$$\int\frac{d\omega}{\pi}(-\omega\mathrm{Im}P^{00}_S(Q))=2\sum_{\mathbf{k}}n_{\mathbf{k}}(\xi_{\mathbf{k}+\mathbf{q}}+\xi_{\mathbf{k}-\mathbf{q}}-2\xi_{\mathbf{k}}), \tag{27}$$

where $n_{\mathbf{k}}=T\sum_{i\omega}G(K)$ and the factor of two arises from summation over pseudo spin indices.

IV. EXTENSION BELOW THE TRANSITION TEMPERATURE

This paper deals exclusively with the normal state. However, it is often convenient to compare and contrast the behavior above and below T_C. Given the mean field form of the normal state self energy Σ_{pg} it is natural to follow earlier work of our own group [4] and of Yang, Rice and Zhang (YRZ) [5] and address the broken symmetry state by taking the full self energy, Σ, to consist of two terms: $\Sigma = \Sigma_{pg} + \Sigma_{sc}$. Here Σ_{sc} is another BCS mean-field like self energy corresponding to the presumed form of the condensate. In this way, there are two different gap parameters: Δ_{sc} and Δ_{pg}.

There are several important distinctions in the way in which these two self energy terms enter into response functions. As suggested in our earlier work [4, 6] for the d-wave pseudogap and for the YRZ case [7], the self energy involving Δ_{pg} should also contain a damping term representing the fact that the non-condensed pairs are not infinitely long lived. This gives rise to the arcs (or spread out nodes) in the case of a d-wave pseudogap.

There are even more important features associated with the sign of the contributions from Δ_{sc} and Δ_{pg} in various response functions, which must guarantee that the superfluid density depends only on the condensate Δ_{sc}; these sign changes appear in the charge density and current density response functions [4, 6]. In a related fashion, the density-density correlation function must include collective mode effects below the transition, in order to be consistent with sum rules.

However, there is no such sign change of Σ_{pg} relative to Σ_{sc} in the spin response, which is not associated with a Meissner effect. Thus in the case of a simple d-wave pseudogap and in the YRZ case as well, one does not expect there to be a significant difference in the spin correlation functions above and below T_C.

By contrast, in the Amperean pairing model [8], it is argued that at T_C the finite wave vector pairing gap converts to a conventional d-wave superconducting phase. This gives rise to a dramatic change in the features associated with neutron scattering. Indeed, a moderate change through the transition is observed in some experiments [9], but, nevertheless, peaks at or near (π, π) are still present. This is in contrast to the rather structureless behavior of the cross section which is found in the Amperean pairing theory reported in this paper.

[1] For simplicity in the text, we will ignore terms that arise from the wave vector dependence of the d-wave gap function. In general this is a small effect. We can see via the sum rule accuracy the importance of including the full wave vector dependence of the d-wave gap. When the wave vector dependence of the gap is ignored, the sum rule accuracy is still very good, but now of the order of 2-3 percent.

[2] L. H. Ryder, *Quantum Field Theory* (Cambridge University Press, 1996), 2nd ed.

[3] D. Bergeron, D. Hankevych, B. Kyung, and A.-M. S. Tremblay, Phys. Rev. B **84**, 085128 (2011).

[4] Q. J. Chen, J. Stajic, S. N. Tan, and K. Levin, Phys. Rep. **412**, 1 (2005).

[5] K.-Y. Yang, T. M. Rice, and F.-C. Zhang, Phys. Rev. B **73**, 174501 (2006).

[6] P. Scherpelz, A. Rançon, Y. He, and K. Levin, Phys. Rev. B **90**, 060506(R) (2014).

[7] P. D. Johnson, H. B. Yang, J. D. Rameau, G. D. Gu, T. E. Kidd, H. Claus, and D. Hinks, Jour. of Phys: Confernce Series **449**, 012007 (2013).

[8] P. A. Lee, Phys. Rev. X **4**, 031017 (2014).

[9] V. Hinkov, P. Bourges, S. Pailhès, Y. Sidis, A. Ivanov, C. D. Frost, T. G. Perring, C. T. Lin, D. P. Chen, and B. Keimer, Nature Physics **3**, 780 (2007).